Available online at www.sciencedirect.com

ScienceDirect

Ceramics International 40 (2014) 4479–4483

CERAMICS INTERNATIONAL

www.elsevier.com/locate/ceramint

Characteristics of hydrolyzed layer and contamination on fused silica induced during polishing

Defeng Liao*, Xianhua Chen, Caixue Tang, Ruiqing Xie, Zhe Zhang

Chengdu Fine Optical Engineering Research Center, Chengdu 610041, China

Received 6 July 2013; received in revised form 27 August 2013; accepted 28 August 2013
Available online 4 September 2013

Abstract

Optical polishing is a chemo-mechanical process which can induce a near-surface hydrolyzed layer with contamination. To date, it is not clear whether the contaminants in the hydrolyzed layer are present as a uniform dopant or as discrete particles. The purpose of the present work is to try to clarify this contamination form. A field emission scanning electron microscope (FE-SEM) was used to determine the micro-topography and composition mapping of the polished fused silica. The relative density of the hydrolyzed layer and the bulk has been assessed using a combination of focused ion beam (FIB) milling and FE-SEM. The results suggest that the dopant contamination is located in the upper layer (tens of nm thick), which has a lower density compared to the bulk. Also, discrete contaminant 'islands' are present in the hydrolyzed layer.

Keywords: Optical polishing; Fused silica; Near-surface hydrolyzed layer; Uniform dopant; 'Islands'-like residuals

1. Introduction

Material removal during polishing takes place because of synergistic chemical and mechanical interactions [1–5]. Characterization of chemistry process has been largely dependent on the measurement of the properties, specifically the thickness, density and hardness, of the hydrolyzed layer on optic surfaces. Investigations in semiconductor CMP processes for planarization of inter-metal dielectric SiO_2 have presented many instructive findings [6]. Nevot and Croce demonstrated the existence of a 2 nm surface region possessing lower density than the bulk, below which the density increased to a value greater than the bulk, gradually returning to the bulk density at a depth of 15–20 nm below the surface [7]. Wallace et al. claimed the presence of a 20 nm compacted region possessing increased density [8]. Trogolo and Rajan revealed chemical/structural modification of SiO_2 to be 100–200 nm from the polished surface and more heavily altered or deformed regions extending to a few tens of nm in depth [9]. In contrary, Tadjiev et al. investigated hydrated extent of silicate glasses by simply exposing them to distilled water at 22 ± 1 °C for various periods of time [10,11]. It is shown that hydration has little if any effect on high durability glasses even at long immersion times. Whereas for low durable glasses hydration reduces the near-surface density, modulus and hardness when compared to the bulk glasses. On the other hand, residual contaminants within hydrolyzed layer have been determined using various means. Adsorption of cerium hydroxide by silica, while tearing away individual silica molecules, also brings residual cerium in the hydrolyzed layer. Kozlowski firstly revealed an exponential decay of contaminant concentration (i.e., Ce) to a depth of 100–200 nm on fused silica surfaces [12]. More recently, Neauport et al. used the inductively coupled plasma atomic emission spectrometer (ICP-AES) to determine the composition and concentrations of HNO_3/HF solution which had etched fused silica, to reveal the contaminant concentrations [13,14]. Secondary ion mass spectroscopy (SIMS) was also employed to determine the concentration of polished-induced contaminants as a function of depth within the hydrated layer. By using SIMS, Liu et al. observed a cerium and iron contaminated layer of approximately 50 nm depth, where the concentration of iron is much higher than that of cerium, on the fused silica surfaces polished with magneto-rheological finishing (MRF) process [15].

Although much work has been done to characterize the hydrolysis process during optical polishing of fused silica, it is still not clear whether the contaminants in the hydrolyzed layer

*Corresponding author. Tel.: +86 288 517 9761; fax: +86 288 517 9749.
E-mail address: defeng_liao@163.com (D. Liao).

0272-8842/$ - see front matter © 2013 Elsevier Ltd and Techna Group S.r.l. All rights reserved.
http://dx.doi.org/10.1016/j.ceramint.2013.08.121

are present in the form of uniform dopant or as discrete particles. In the present work, FE-SEM has been used to determine the micro-topography and composition mapping of the polished fused silica surface. Combined with the milling function of the FIB, composition of the hydrolyzed layer has also been determined. The results will be systematically analyzed.

2. Experimental

The Helios NanoLab™ 650 system including FE-SEM, FIB and their combined use was employed. Its through-the-lens detector possesses highest collection efficiency of secondary electrons (SE) and on-axis backscattered electrons (BSE). During SEM analysis, electrons are emitted onto the specimen surface yielding various output signals. SE are the scattered atomic electrons of the specimen from the near-surface region within several nanometers [16]. Collection of SE presents the topography, in micro- and nano-scales, of the specimen. BSEs result from the bounce of primary electrons by atomic nucleus of the specimen within the depth of several hundreds of nanometers. An important utility of BSE signal is composition mapping. The BSE intensity increases with atomic number, yielding brighter images [16].

Fused silica and K9 glass samples ($\Phi 25 \times 5$ mm) were polished on a continuous polisher using a polyurethane pad (GR-35 by Universal Photonics Inc.). Fused silica contains higher than 99.9 wt% SiO_2 in terms of silicate tetrahedrons. Whereas the extensively used alkaline K9 glass generally comprises 69.13% SiO_2, 10.75% B_2O_3, 0.36% As_2O_3, 3.07% BaO, 10.40% Na_2O, and 6.29% K_2O. Some samples then underwent wet etching of hydrofluoric acid removing a depth of 1 μm. Both polished and etched samples were detected using FE-SEM in the modes of SE and BSE, respectively. A Pt layer was initially plated on the other fused silica samples so as to prevent the hydrolyzed layer from damage by scattered ions. FIB was, then, used to mill a dent on the plated surface with a depth of several microns. Afterwards, FE-SEM focuses on the cross-section of the dent to determine composition mapping of the layer in the mode of BSE.

3. Results and analysis

Fig. 1(a)–(c) shows the composition mapping of the milled near-surface layers of polished fused silica, etched fused silica and polished K9 glass, respectively. The upper layer (right side in the images) is the sputtered platinum. In Fig. 1(a), the hydrated layer is obvious, with a thickness of less than 100 nm, below the platinum layer in lighter contrast. Furthermore, the brightness of this layer in SEM image decreases as the depth increases until the pristine zone. This indicates that the hydrated layer has a reduced density when compared to the bulk silica, and further, the reduced density increase as the layer approaches to the pristine zone. It is suggested that extent of hydrolyzation decreases as the depth is increased. The results are consistent with the investigation conducted by

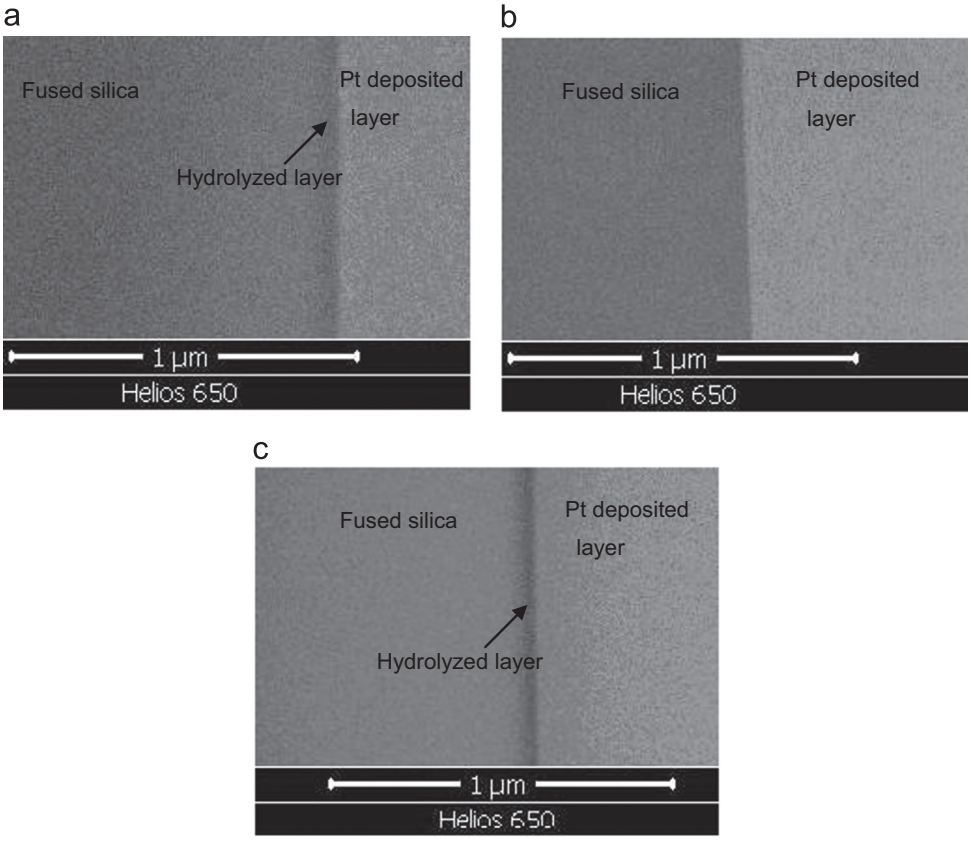

Fig. 1. Cross-section near the top surface of polished fused silica. (a) Polished surface of fused silica;, (b) Etched surface of fused silica and (c) Polished surface of K9 glass.

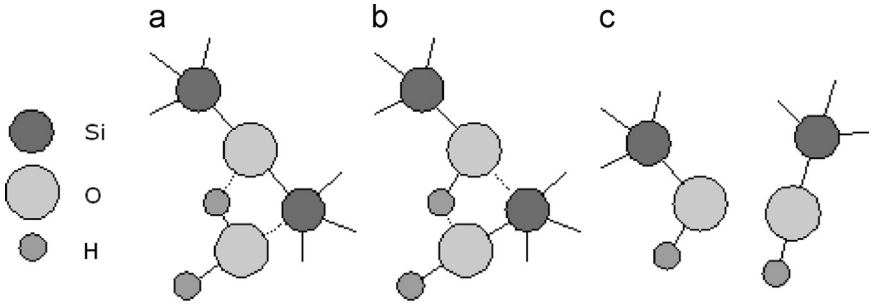

Fig. 2. An illustration of the hydration process of the siloxane and water.

Mansurov et al. [17]. They have expressed composition of the hydrated layer in terms of nonstoichiometric hydroxyl, $SiO_x(OH)_y$. Based on their determination by deep ultraviolet and infrared spectra, coefficient y lies between 1 and 2 on the surface, and gradually approaches to 0 with the increasing depth. Fig. 1(b) shows that the hydrolyzed layer has been completely removed by the etching process. It is demonstrated that hydrofluoric acid etching is an effective means to remove the modified layer. Comparing Fig. 1(a) and (c), one can notice that the hydrolyzed layer on K9 glass is much thicker and clearer than that of fused silica. This is due to their difference in composition and thus the chemical durability.

Material removal during polishing can be divided into three stages: breakage of the silica network forming (Si–O–H), reduction of CeO_2 to Ce_2O_3 and the interaction of the both. Silica hydrolysis involves interactions between siloxane bonds (Si–O–Si) and water. The reaction for the breakage of the silica network to form a hydrated surface includes several steps, as shown in Fig. 2 [9,18]. Initially, an ambient water molecule could attach to the Si–O–Si bond by forming a hydrogen bond between its hydrogen and the oxygen atom in the silica surface, while lone pair orbitals of the oxygen from water interact with the Si atoms. Then, hydrogen bound to water transfers a proton to the oxygen of silica, and an electron is simultaneously transferred from the oxygen of water to the Si atom. Finally, two new bonds are formed (Si–O–H), by destroying the original siloxane bond. The dissolution of silica occurs if all four bridging oxygen bonds are hydrated, forming the solute species $Si(OH)_4$ (silanol) [19,20]. The reaction rate is believed to be controlled by the diffusion of water into silica structure and also be heavily dependent of pH value of the polishing slurry. Investigations revealed that, during CMP of dielectric silica using silica slurry, the dissolution process of silica accelerates significantly with increasing pH value from 2 to 11 and pressure from 50 to 250 MPa [21,22].

On the other hand, the redox (reduction/oxidation) processes at the ceria particle surface could contribute to the chemical reactivity of the ceria particles [23]. CeO_2 was reported to be thermodynamically unstable in aqueous environments. The reduction process of CeO_2 to Ce_2O_3 (i.e., from Ce^{4+} to Ce^{3+}) occurs during the production of oxygen vacancies and the localization of an electron [24]. The electron energy-loss spectroscopy analysis shows a gradual increase of Ce^{3+} with increasing distance from the particle center [25]. It is revealed that the tri-valent cerium Ce^{3+} is strongly segregated to within $\sim$1 nm of the surface rather than Ce^{4+} observed $\geq$2 nm away from the surface [26,27]. Indeed, during polishing, the ceria particles consist of a mixed valence state of predominantly Ce^{4+} in the interior and Ce^{3+} at the surface. It is well established that when exposed to water, oxide surfaces acquire surface hydroxyls through interaction between the surface metal and oxygen atoms and adjacent water molecules, as shown in Eq. (1) [28–30]. Taking ceria as an example, the reaction proceeds as shown in Eq. (2). Ce_2O_3 in the form of $=$ Ce–OH at the surface of ceria particles would have the basic reaction as shown in Eq. (3) [19,31]. Cerium hydroxide Ce_2O_3 condenses with the glass surface (silanol surface) to form a Ce–O–Si bond. The bond strength of this new oxide is stronger than that of the Si–O–Si bond (i.e., glass). Hence the ceria particle essentially tears away individual silica molecules [31].

$$–M+–MO+H_2O\rightarrow –MOH+–MOH \quad (1)$$

$$=Ce-O-Ce\equiv +H_2O\rightarrow =Ce-OH+HO–Ce= \quad (2)$$

$$=Ce-OH+HO-Si\equiv \rightarrow =Ce-O-Si\equiv +H_2O \quad (3)$$

The difference in hydrated layer thicknesses of K9 and fused silica can be ascribed to hydration kinetics and chemistry. In fused silica, the weight percentage of SiO_2 with a form of asilicate tetrahedrons exceeds 99.9%. Whereas K9 glass generally comprises 69% SiO_2 and other 31% alkali and alkaline earth oxides such as Na_2O and K_2O. Alkali and alkaline earth ions outside the dominant Si–O network remarkably promote the chemical reactivity. As a network modifier, Na_2O could open up the silica network by breaking some of the Si–O bonds in the network, which leads to low viscosity and poor chemical durability (see Eq. (4)). Sodium hydroxide (NaOH) resulting from the exchange of sodium ions in glass for hydrogen ions in water accelerates the corrosion rate of the silicate network, as shown in Eqs. (4) and (5) [32]. Therefore, alkali silicate glasses have a lower resistance to aqueous corrosion than fused silica. Izumitani et al. have found that removal rate of K9 was four times that of fused silica [33].

$$\equiv Si-O-Na+H_2O\rightarrow \equiv Si-OH\downarrow +NaOH \quad (4)$$

$$\equiv Si-O-Si\equiv +NaOH\rightarrow \equiv Si–OH\downarrow +Na-O-Si\equiv \quad (5)$$

Fig. 3 shows micro-topography and composition mapping of the polished fused silica determined using FE-SEM in the mode of SE and BSE, respectively. It is well known that the

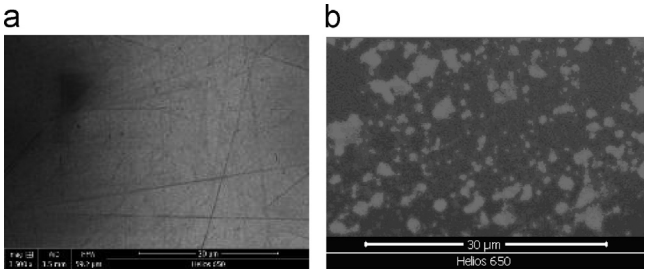

Fig. 3. FE-SEM determination of the polished fused silica. (a) Micro-topography in the mode of SE. (b) Composition mapping in the mode of BSE.

SE mode is used to observe the micro-topography and the BSE mode could show the composition variations. Fig. 3(a) revealed several shallow scratches present on the polished surface. These shallow scratches are most likely to be plastic scratches, resulting from plastic cutting by individual or aggregated abrasives during polishing. As established in the literature, material removal during polishing generally involves several aspects, including mechanical abrasion [1], chemical reaction [2], surface melting and adhesion [34]. These shallow scratches suggest validation of the abrasion mechanism, which claims that the material was removed by a plastic cutting process involving the action of the abrasive particles [35]. In previous studies, submicron sized grooves on polished surfaces have also been demontrated by atomic force microscopy (AFM) [36–38].

Fig. 3(b) shows composition mapping of the polished surface of fused silica. Various 'island' type residuals with irregular shapes are present on the surface. The lower brightness of these residuals indicates that the atomic number or density is larger than that of the bulk SiO_2. Thus they are most likely to be residual cerium oxides. Investigations conducted by Abiade have also revealed these 'islands' residuals and confirmed that the 'islands' are actually cerium-rich [36]. According to the previously described material removal process, the adsorption of silanol surface by cerium hydroxide brings residual cerium in the hydrolyzed layer while tearing away individual silica molecules. In this case the hydrolyzed silica surface in the form of silanol serves as the adsorbent and the abrasive particle serves as the adsorbate. Then, combined with the effect of surface melting and adhesion, some absorbed cerium oxide clutches are most likely to be immersed in the hydrolyzed layer.

4. Conclusions

By using FE-SEM, a hydrolyzed layer with a depth of tens to one hundred nm has been confirmed on the polished fused silica. Compared to the bulk silica, the hydrated layer has a reduced density and it increases as the layer approaches to the pristine zone. Chemical etching has been proven to be an effective means to remove the hydrolyzed layer. The hydrolyzed layer on polished K9 glass is much thicker, which can be ascribed to the lower chemical durability and higher reactivity. Shallow plastic scratches on the polished fused silica surface could demonstrate the validation of abrasion mechanism for material removal. The 'islands'-like residuals are presented with lower brightness in the FE-SEM image, and these 'islands' are residual ceria clusters as absorbed by silica.

References

[1] J.Y. Lai, Mechanics, mechanisms, and modeling of the chemical mechanical polishing process (Ph.D. dissertation), Massachusetts Institute of Technology, 2001.
[2] J.T. Abiade, Characterization of the chemical effects of ceria slurries for dielectric chemical mechanical polishing (Ph.D. dissertation), University of Florida, 2004.
[3] D.F. Liao, R.Q. Xie, J. Hou, X.H. Chen, B. Zhong, A polishing process for nonlinear optical crystal flats based on an annular polyurethane pad, Applied Surface Science 258 (22) (2012) 8552–8557.
[4] D.F. Liao, H. Zhao, Z.G. Yuan, R.Q. Xie, Improvement of Surface Figure in the Polyurethane Pad Continuous Polishing Process, Applied Mechanics and Materials 319 (2013) 107–112.
[5] D.F. Liao, Z.G. Yuan, C.X. Tang, R.Q. Xie, X.H. Chen, Mid-spatial Frequency Error (PSD-2) of optics induced during CCOS and full-aperture polishing, Journal of the European Optical Society—Rapid Publications 8 (2013) 13031.
[6] T. Hoshino, Y. Kurata, Y. Terasaki, K. Susa, Mechanism of polishing of SiO_2 films by CeO_2 particles, Journal of Non-Crystalline Solids 283 (1–3) (2001) 129–136.
[7] L. Nevot, P. Croce, Caracterisation des surface par reflexion rasante de rayons X. Application a l'etude du polissage de quelques verres silicates, Revue de Physique Appliquée 15 (1980) 761–779.
[8] W.E. Wallace, W.L. Wu, R.A. Carpio, Chemical–mechanical polishing of SiO_2 thin films studied by X-ray reflectivity, Thin Solid Films 280 (1–2) (1996) 37–42.
[9] J.A. Trogolo, K. Rajan, Near surface modification of silica structure induced by chemical/mechanical polishing, Journal of Materials Science 29 (17) (1994) 4554–4558.
[10] D.R. Tadjiev, R.J. Hand, Surface hydration and nanoindentation of silicate glasses, Journal of Non-Crystalline Solids 356 (2) (2010) 102–108.
[11] D.R. Tadjiev, R.J. Hand, P. Zeng, Comparison of glass hydration layer thickness measured by transmission electron microscopy and nanoindentation, Materials Letters 64 (9) (2010) 1041–1044.
[12] M.R. Kozlowski, J. Carr, I. Hutcheon, R. Torres, L. Sheehan, D. Camp, M. Yan, Depth profiling of polishing-induced contamination on fused silica surfaces, in: Proceedings of a Symposium Sponsored by the American Society for Testing and Materials and by the National Bureau of Standards, Laser Induced Damage in Optical Materials, Society of Photo-Optical, vol. 3244 1997.
[13] J. Neauport, L. Lamaignere, H. Bercegol, F. Pilon, J.C. Birolleau, Polishing-induced contamination of fused silica optics and laser induced damage density at 351 nm, Optics Express 13 (25) (2005) 10163–10171.
[14] J. Neauport, P. Cormont, L. Lamaignere, C. Ambard, F. Pilon, H. Bercegol, Concerning the impact of polishing induced contamination of fused silica optics on the laser-induced damage density at 351 nm, Optics Communications 281 (14) (2008) 3802–3805.
[15] Z.J. Liu, S.Y. Li, Z. Wang, X.Q. Peng, Research on the subsurface damage during finishing for optics, Aviation Precision Manufacturing Technology 44 (5) (2008) 1–4.
[16] J.B. Bindell, in: C.R. Brundle, C.A. Evans Jr., S. Wilson (Eds.), Encyclopedia of Materials Characterization: Surfaces, Interfaces, Thin Films, Butterworth-Heinemann, Professional Publishing, Boston, Gulf, 1992, p. 699.
[17] G.M. Mansurov, R.K. Mamedov, A.S. Sudamshkln, Study of the nature of a polished quartz–glass surface by ellipsometric and spectroscopic methods, Optics and Spectroscopy (USSR) 52 (5) (1982) 509–513.
[18] G.B. Basim, Formulation of engineered particulate systems for chemical mechanical polishing applications (Ph.D. dissertation), University of Florida, Gainesville, FL, 2002.

[19] L. Cook, Chemical processes in glass polishing, Journal of Non-Crystalline Solids 120 (1990) 152–171.
[20] J.A. Trogolo, K. Rajan, Near surface modification of silica structure induced by chemical/mechanical polishing, Journal of Materials Science 29 (17) (1994) 4554–4558.
[21] R.K. Iler, The Chemistry of Silica: Solubility, Polymerization, Colloid and Surface Properties, and Biochemistry, Wiley, New York, 1979.
[22] S. Ito, M. Tomozawa, Stress corrosion of silica glass, Journal of the American Ceramic Society 64 (11) (1981) C-160.
[23] R. Sabia, H.J. Stevens, Performance characterization of cerium oxide abrasives for chemical-mechanical polishing of glass, Machining Science and Technology 4 (2) (2000) 235–251.
[24] N.V. Skorodumova, S.I. Simak, B.I. Lundqvist, I.A. Abrikosov, B. Johansson, Quantum origin of the oxygen storage capability of ceria, Physical Review Letters 89 (16) (2002) 166601-1.
[25] S.R. Gilliss, J. Bentley, C.B. Carter, Nanochemistry of Ceria Abrasive Particles, in: Proceedings of Materials Research Society Symposium-Proceedings, San Francisco, Materials Research Society, vol. 818, 2004, pp. 9–14.
[26] J. Bentley, S.R. Gilliss, C.B. Carter, J.F. Al-Sharab, F. Cosandey, I.M. Anderson, P.J. Kotula, Nanoscale EELS analysis of oxides: composition mapping, valence determination and beam damage, Journal of Physics Conference Series. IOP Publishing 26 (1) (2006) 69–72.
[27] S.R. Gilliss, J. Bentley, C.B. Carter, Electron energy-loss spectroscopic study of the surface of ceria abrasives, Applied Surface Science 241 (1) (2005) 61–67.
[28] K. Osseo-Asare, Surface chemical processes in CMP Relationship between silica material removal rate and the point of zero charge of the abrasive material, Journal of the Electrochemical Society 149 (12) (2002) G651–G655.
[29] W. Stumm, Chemistry of the Solid–Water Interface: Processes at the Mineral–Water and Particle–Water Interface in Natural Systems, Wiley, New York, 1992.
[30] G.A. Parks, The isoelectric points of solid oxides, solid hydroxides, and aqueous hydroxo complex systems, Chemical Reviews 65 (2) (1965) 177–198.
[31] T.I. Suratwala, M.D. Feit, W.A. Steele, Material removal and surface figure during pad polishing of fused silica, Journal of the American Ceramic Society 93 (5) (2010) 1326–1340.
[32] M.J. Cumbo, Chemo-mechanical interactions in optical polishing (Ph.D. dissertation), University of Rochester, Rochester, New York, 1993.
[33] T. Izumitani, S. Adachi, Polishing Mechanism of Fused Silica Glass, Science of Polishing Topical Meeting, Monterey CA, Paper TuB-A1–1, 1984.
[34] E. Rabinowicz, Polishing, Scientific American 218 (1968) 91–99.
[35] L. Lu, Formation of wear particles in polishing of brittle solids and grinding of metals (Ph.D. dissertation), Purdue University, 1995.
[36] A.A. Tesar, B.A. Fuchs, P.Paul Hed, Examination of the polished surface character of fused silica, Applied Optics 31 (34) (1992) 7164–7172.
[37] J.M. Bennett, J. Jahanmir, J.C. Podlesny, T.L. Balter, D.T. Hobbs, Scanning force microscope as a tool for studying optical surfaces, Applied Optics 34 (1) (1995) 213–230.
[38] A. Duparre, J. Ferre-Borrull, S. Gliech, G. Notni, J. Steinert, J.M. Bennett, Surface characterization techniques for determining the root-mean-square roughness and power spectral densities of optical components, Applied Optics 41 (1) (2002) 154–171.